TSUNAMI SIMULATION USING DYNAMIC GROUND DISPLACEMENT DUE TO SEISMIC FAULTING

Tatsuo OHMACHI[1], Hiroshi TSUKIYAMA[2] And Hiroyuki MATSUMOTO[3]

SUMMARY

In conventional tsunami simulation technique, several kinds of simplification have been employed, but they should be reconsidered in the light of the state-of-the-art technology, because considerable discrepancy between numerical simulation and actual observation is often pointed out regarding, for example, arrival time and wave height. As for the simplification, effects of dynamic ground displacement of the seafloor are disregarded in comparison with those of static (or residual) one associated with seismic faulting, and the water is assumed to be incompressible regardless of its acoustic effects. In the present study, tsunami simulation is conducted without using these two kinds of simplification, taking into account both the dynamic displacement and acoustic effects. As a result, the tsunami simulated with the dynamic displacement is found to be remarkably larger in the wave height especially in near-field where these two effects are superposed. In far-filed, however, the two kinds of simulated tsunamis are likely to show little difference in the wave height, but to show considerable difference in the arrival time. In addition, it is often the case in the dynamic simulation that the first arrival of tsunami is the ebb.

INTRODUCTION

Recently, serious disasters have been caused by tsunamis around the world, and any possible effort needs to be urgently made to mitigate future tsunami disasters. According to conventional tsunami simulation technique, the initial sea surface disturbance is assumed to be the same as the residual displacement caused by seismic faulting, and wave propagation is approximated with long waves. In recent years, we have developed an advanced tsunami simulation technique, and simulated tsunami generation followed by propagation as exactly as possible, without using the conventional approximation, because, with the technique, we aim to contribute to tsunami warning system to improve the accuracy.

There are important problems still unsolved in the boundary areas of earthquake engineering and coastal engineering. For example, there is a large discrepancy between fault models of an earthquake, estimated from different data, such as seismic wave data and tsunami data. The discrepancy may be attributed to the above-mentioned approximation. To reduce this kind of discrepancy, we apply our technique to simulate actual tsunami due to the 1993 Hokkaido-Nansei-oki, Japan, earthquake by using a seismically determined fault model.

[1] *Department of Built Environment, Tokyo Institute of Technology, Japan Email: ohmachi@enveng.titech.ac.jp*
[2] *Tsukiyama Research, Inc.,Japan Email: pxi10213@niftyserve.or.jp*
[3] *Department of Built Environment, Tokyo Institute of Technology, Japan Email: matsumo@enveng.titech.ac.jp*

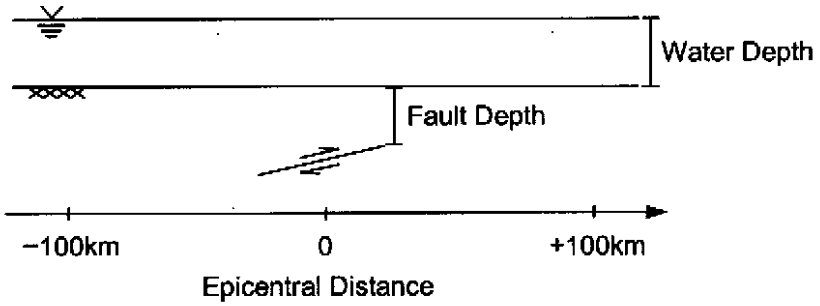

Figure 1: Tsunami analysis model

Table 1: Fault parameters and velocity model of ground

Width	30km
Fault depth	7km
Dip	30degree
Dislocation	10m
Rupture velocity	3.0km/sec
Rise time	2.0sec
Vp	7.0km/sec
Vs	4.0km/sec

PROCEDURE

In the present study, seafloor and fluid body are assumed to have no interaction. Based on this assumption, the generation and propagation of tsunami is simulated by imposing the velocity of dynamic ground displacement resulting from seismic faulting as an input to fluid domain at the seafloor (e.g. Ohmachi and Nakama, 1997). We call this procedure 'Dynamic Analysis', in contrast with conventional static procedure in which the dynamic effects are neglected. Two-step analyses are involved in the present dynamic analysis; the first step is to simulate the dynamic ground displacement due to seismic faulting, and the second step is to simulate the generation and propagation of tsunami. The first analysis of the ground displacement is simulated by means of boundary element method (BEM), because of easy modeling of irregular seafloor as well as seismic source. The second analysis of the fluid domain is simulated by means of finite difference method (FDM). The Navier-Stokes equations are used as a governing equation for the fluid analysis without using long wave approximation. The effect of acoustic wave is included in the numerical simulation to take account of sound velocity into the mass conservation equation.

DIMENSIONAL TSUNAMI SIMULATION

Features of Dynamic Analysis

The effect of dynamic ground displacement on tsunami generation and propagation is evaluated by simulating simple tsunamis in 2-dimension. A thrust faulting with constant rupture velocity in an elastic half-space is considered (see Figure 1). Parameters of the fault and the ground are shown in Table 1. Figure 2 shows analytical results in the case of water depth 3000m. The lower surface and the upper surface represent the sea floor and the sea surface, respectively in the figure.

In Figure 2, the snapshots after the fault rupturing at every 5 seconds until 30 seconds are shown. At 10 seconds after the rupturing, the maximum uplift of 789cm occurs around the near-field, which is 1.7 times as large as the residual displacement. At 15 seconds, the Rayleigh wave generates in the near-filed (see A) and propagates along the seafloor to the right in the figure. Thus, in the near-field, dynamic ground displacement is lager than that of residual one, because of superposition of the high wave induced by the Rayleigh wave.

As regards sea surface disturbance, there is time delay in the dynamic analysis in comparison with conventional one, because of elapsed time in fault dislocation and wave propagation from the seafloor to the sea surface. At

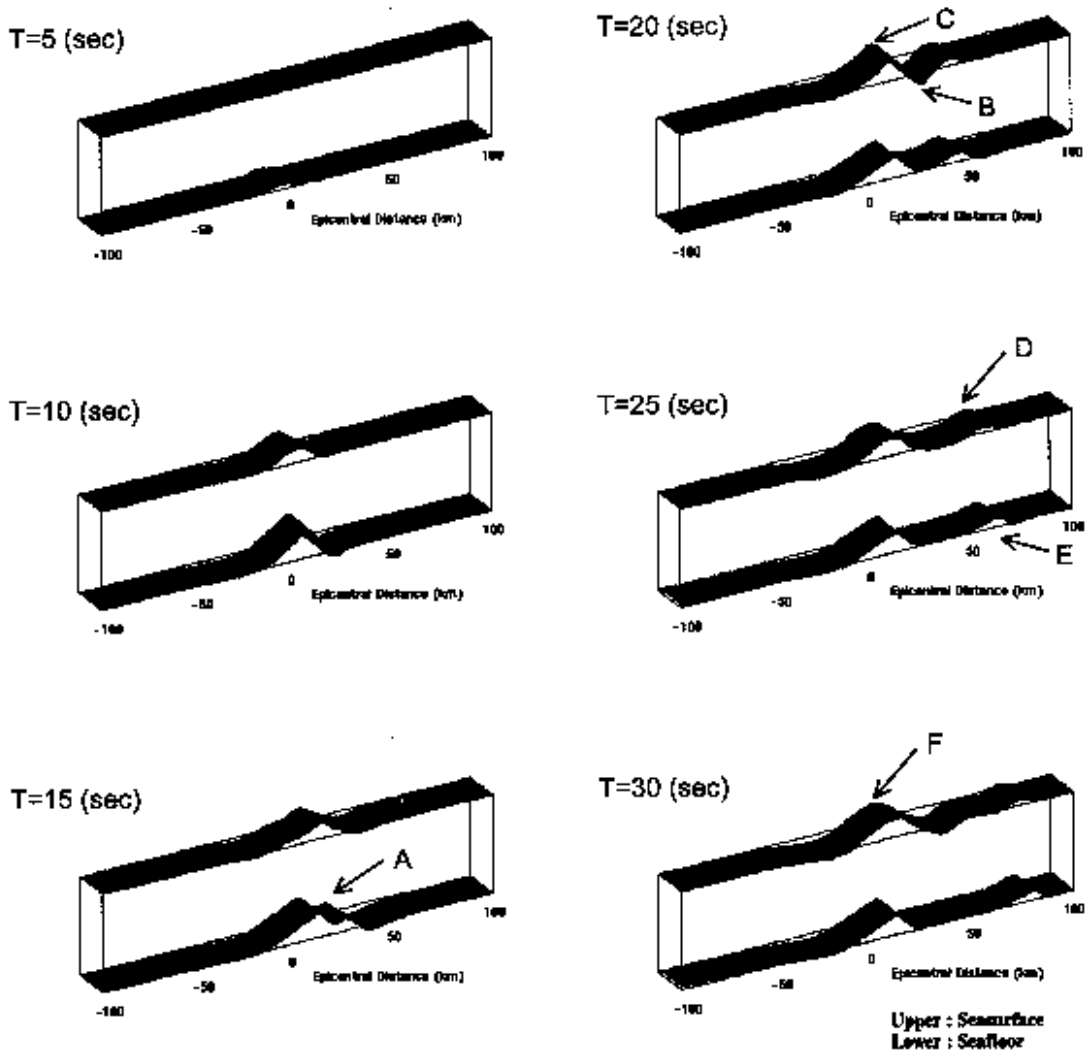

Figure 2: 2-dimensional tsunami simulation

20 seconds, a single peak of the sea surface is divided into two peaks, producing a sharp fall between the two peaks (see B). The displacement of the first peak is larger than that of residual one of the ground (see C). As regards wave propagation, sea wave with velocity higher than tsunami can be seen (see D). This wave is due to Rayleigh wave propagating along the seafloor (see E). The Rayleigh wave shows a large amplitude on the right side of the figure, but a small amplitude on the left side. Likewise the sea wave induced by Rayleigh wave has similar characteristic. This sea wave induced by Rayleigh wave has a period shorter than that of tsunami. On the other hand, tsunami simulated by means of the dynamic analysis (see F) is propagated with velocity and amplitude similar to those from conventional analysis.

Tsunami Generation Induced by Dynamic Ground Displacement

Using the model shown in Figure 1, the maximum wave height in the near-field is evaluated by changing rise time of the fault rupturing from 0.5seconds to 20seconds, as well as water depth is changed from 100m to 3000m.

Figure 3 compares the maximum water displacements Ws with the residual displacement Ds during 30 minutes after the fault rupturing, when water depth is 100m or 3000m. According to the present dynamic analysis, when water depth is kept constant, the smaller the rise time becomes, the larger the difference between Ws and Ds becomes. On the contrary, when the rise time is kept constant, the smaller the water depth becomes, the larger the difference between Ws and Ds becomes. This suggests that it is necessary to consider the effect of dynamic ground displacement especially in the neighboring sea with shallow water. As for the water displacement on the right side from the peak in Figure 3, the larger the water depth becomes, the larger the water displacement appears conversely, because the period of Rayleigh wave propagating along the seafloor becomes much closer to the natural period of fluid associated with water depth.

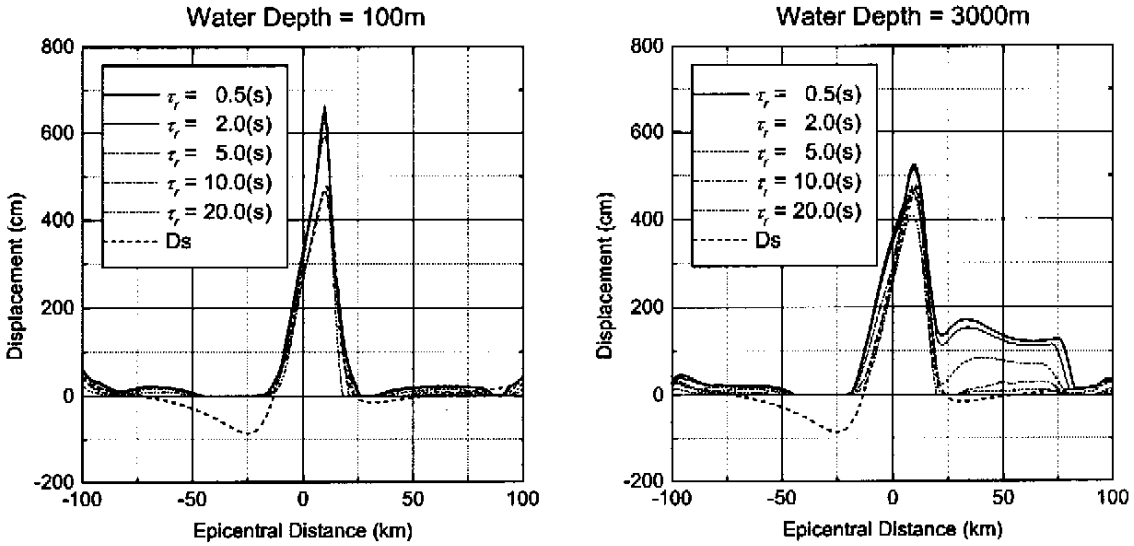

Figure 3: Distribution of maximum water displacement and residual displacement

TSUNAMI SIMULATION OF THE 1993 HOKKAIDO-NANSEI-OKI, JAPAN, EARTHQUAKE

Fault Model and Calculation Models

The 1993 Hokkaido-Nansei-oki, Japan, earthquake (Mw=7.5) occurred at 13:17 GMT on 12 July 1993, in a close proximity to Okushiri Island, southwest of Hokkaido. This earthquake triggered a giant tsunami that caused serious damage and numerous casualties. The fault model of this earthquake has not been determined yet, because the rupture process and distribution of aftershocks were very complex (e.g. Kakehi and Irikura, 1997). Different fault models were presented based on different data, such as seismic data, tsunami data, and geodetic data. For example, a fault model from inversion analysis of tsunami data, mainly tidal records, has large dislocation and a steep dip angle (e.g. Takahashi et al., 1994). Between this fault model and another fault model estimated from seismic data and distribution of aftershocks, there are lager discrepancies.

In the present study, we analyzed the 1993 Hokkaido-Nansei-oki, Japan, earthquake tsunami, employing a seismic fault model estimated from strong ground motions recorded within 400km of epicenter and vertical P waveforms at teleseismic distance (e.g. Mendoza and Fukuyama, 1996). As shown in Table 2 and Figure 4, this fault model is composed of three fault planes; the Northern, the Southern, and the Local faults.

Figure 4 shows the location of the fault planes and the calculation area of the dynamic analysis. The calculation area covers 220km×200km in NS and EW directions, respectively, which includes the fault planes. The grid size of BEM used for analysis of dynamic ground motion is 4km, and the frequency range for the analysis is between 0 and 2Hz. The rupture process starts at 0 second for the Northern fault, at 23.3 seconds for the Southern fault, and at 46.6 seconds for the Local fault. Each rupture stars at the bottom line of the fault, and propagates upwards. Until 128 seconds after the fault rupturing, the calculated velocity of the ground is induced at the bottom of fluid domain.

In the calculation of fluid domain, the grid seize and time step are set to 4km and 0.25 seconds, respectively, in order to keep stability of calculation by FDM. The boundary conditions are of complete wave-reflecting boundary both along coastlines and the open sea. Our model can not account for runup for the time being.

Simulation of Dynamic Ground Motion

Figure 5 shows the snapshots of ground motion displacement at 20, 40, 60, and 100 seconds after the fault rupturing. At 20 seconds, the uplift occurs just above the Northern fault. At 40 seconds, the Rayleigh wave from the Northern fault reaches southwestern Hokkaido (see R_N). The width of this Rayleigh wave is fairly coincident with fault length of the Northern fault. At this moment, the uplift has occurred just above the Southern fault caused by stating the Southern fault rupturing. At 60 seconds, there is a large uplift on the western side of Okushiri Island. At this moment, the Rayleigh wave from the Southern fault reaches southwestern Hokkaido (see R_S). The width of this Rayleigh wave is also fairly coincident with fault length of the Southern fault. The Rayleigh waves from both the faults appear to propagate only on the eastern side. These characteristics of Rayleigh waves are referred to as directivity. At 100 seconds, the deformation of the seafloor approaches residual

Table 2: Fault parameters of the 1993 Hokkaido-Nansei-oki, Japan, earthqual

	North	South	Local
Seismic moment (N*m)	$2.04*10^{20}$	$1.36*10^{20}$	$0.63*10^{20}$
Length (km)	110	90	30
Width (km)	70	70	20
Depth (km)	5	2	2
Strike (degree)	200	160	160
Dip (degree)	30	30	60
Angle (degree)	100	90	90
Dislocation (m)	0.76	0.72	3.00
Rupture velocity (km/sec)	3.0	3.0	3.0
Rise time (sec)	3.0	4.5	4.5

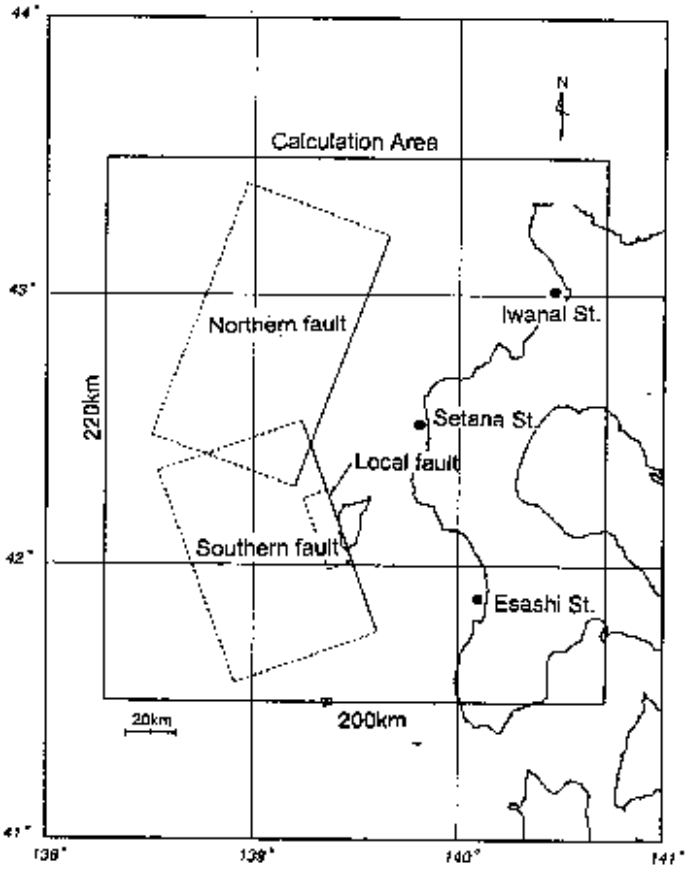

Figure 4: Fault planes location and calculation area

displacement, showing that Okushiri Island subsides by some 10cm (see S). This subsidence of Okushiri Island obtained by the dynamic analysis corresponds well with that measured by GPS (e.g. Hashimoto et al., 1994). And there is an uplift of more 100cm on the western side of Okushiri Island (see U).

Tsunami Simulation

Figure 6 shows the snapshots of a tsunami simulation process at 20, 40, 60, and 80 seconds after the fault rupturing. The two sea waves induced by Rayleigh waves arrive at the southwestern coast of Hokkaido at 40 seconds (see R_N') and at 60 seconds (see R_S'), respectively. And then, these two waves become overlapped and arrive at Esashi station at 60 seconds. At Iwanai station, these two waves arrive at 45 seconds and 80 seconds, respectively. The sea surface disturbance from 60 to 80 seconds after the rupturing corresponds well with that of higher runup found at the western coast of Okushiri Island.

Figure 7 shows the snapshots of tsunami propagation at every 100 seconds from 300 to 800 seconds after the

fault rupturing. At 300 seconds, the tsunami arrives at the southwestern coast of Hokkaido. This arrival time is in

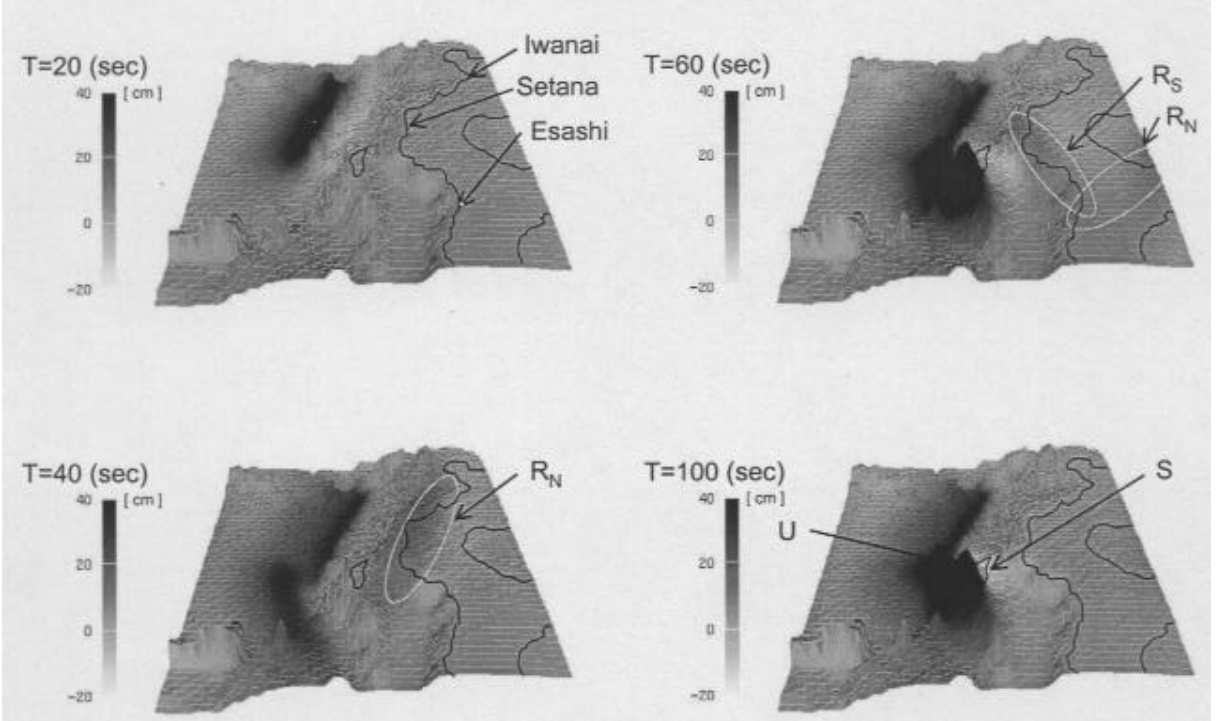

Figure 5: Ground motion of seafloor

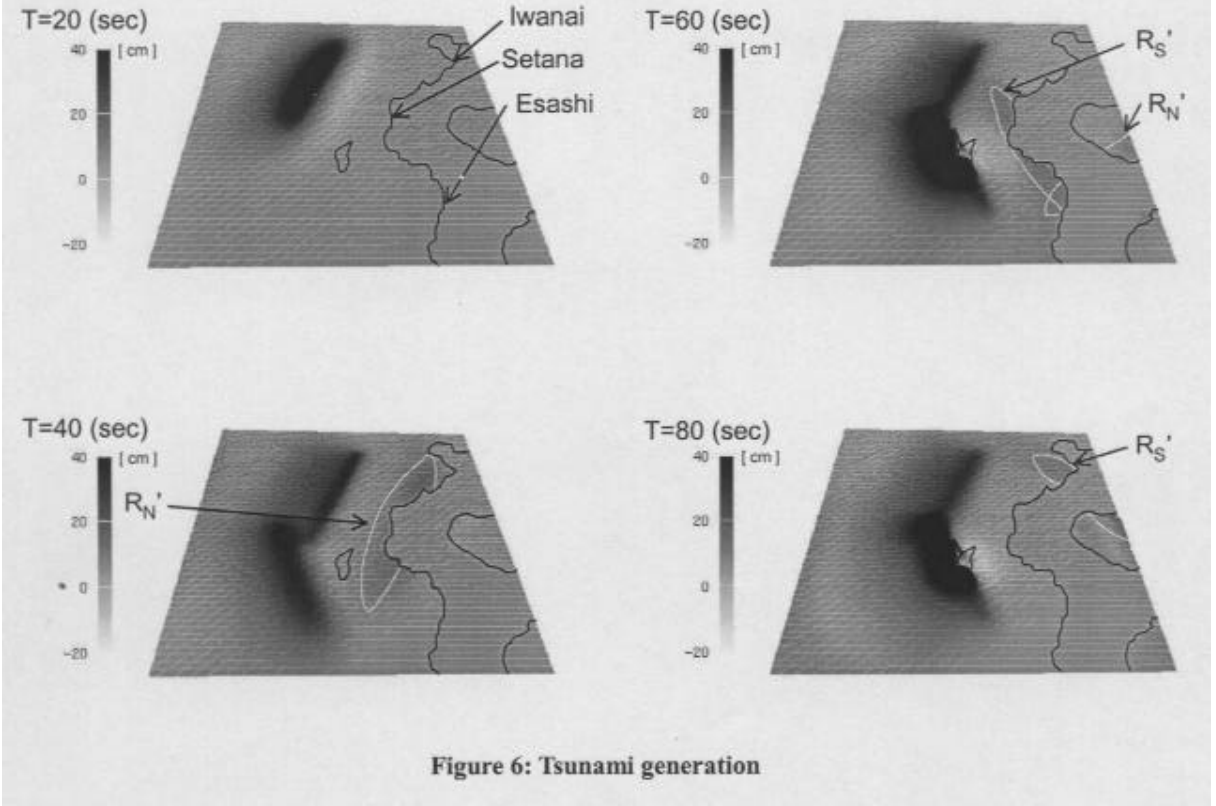

Figure 6: Tsunami generation

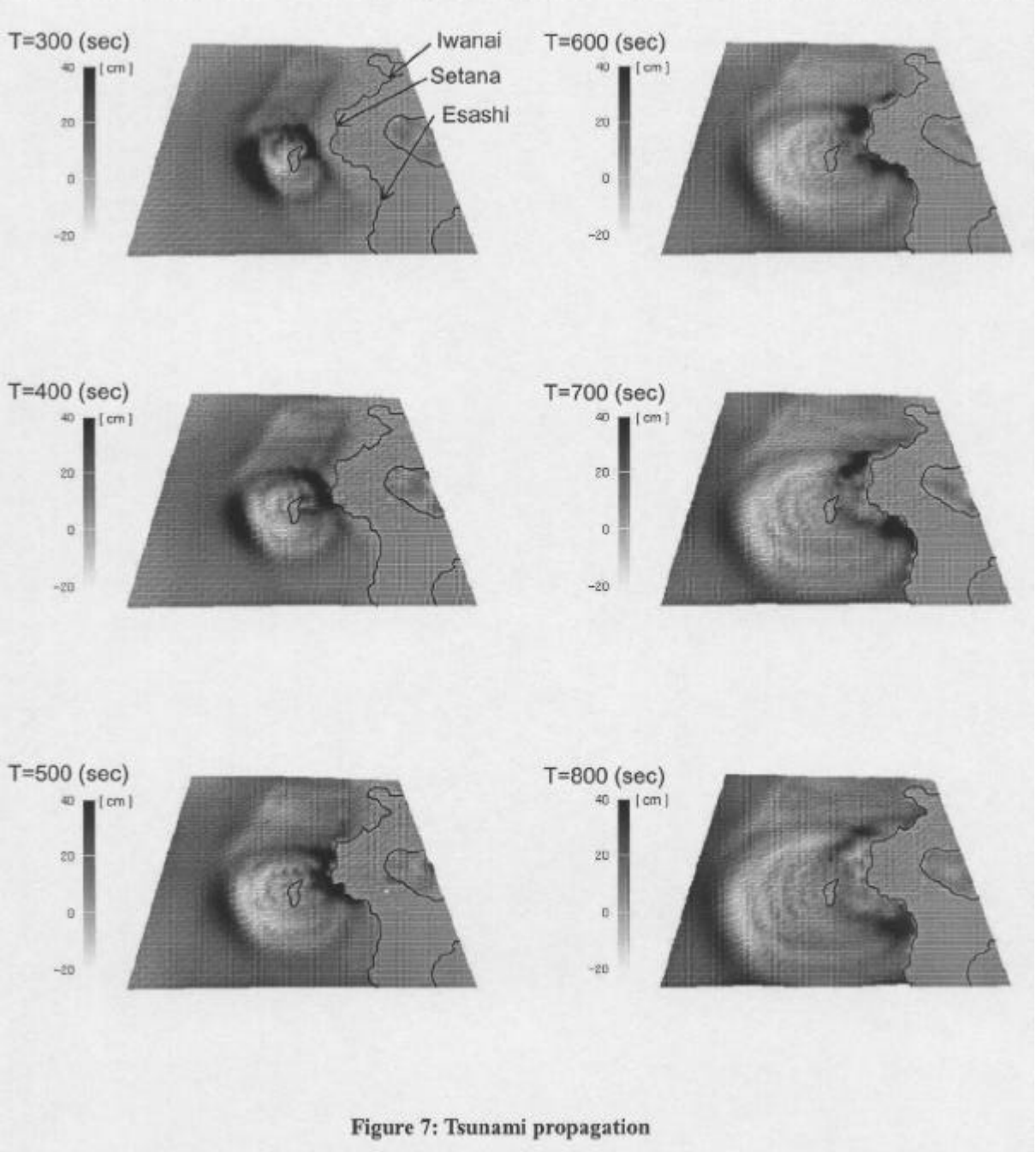

Figure 7: Tsunami propagation

agreement with the witnesses there. The tsunamis from both the Northern fault and the Southern fault come together around Setana station, and separate toward north and south each other at 600 seconds. The first tsunami arrives at Iwanai station at 800 seconds and the maximum height takes place at 900 seconds. Arrival time of the first tsunami witnessed at Iwanai station was at 900 seconds. There is a good agreement between the dynamic analysis and the witnesses. On the other hand, the tidal record at Esashi station indicates the ebb at the first arrival of the tsunami. From the dynamic analysis, there is a little ebb for the first tsunami at Esashi station. Using the present dynamic analysis, the first tsunami in near-field tends to be the ebb.

There were many witnesses, stating that the first tsunami was small along the southwestern coast of Hokkaido. Shuto and Matsutomi (1995) suggested that there might be another tsunami generation mechanism in addition to the major fault movement. This small first tsunami may be the sea wave induced by Rayleigh wave, as simulated with the dynamic analysis. In addition, the sea wave induced by Rayleigh wave shows spacial directivity like Rayleigh wave itself. According to the dynamic analysis, the sea wave of 15cm amplitude induced by Rayleigh wave arrives at Esashi station at about 540 seconds, and arrives at Iwanai station at about 700 seconds before the first tsunami arrives. The tidal records at both Esashi and Iwanai stations located in front of the fault indicate sea

surface disturbance of 40cm amplitude, while the tidal record at Rumoi station located aside to the fault does not indicate such disturbance. These observations are in a good agreement with the dynamic analysis.

CONCLUSION

The following conclusions can be drawn from the present dynamic analysis.

(1) The effect of the dynamic ground displacement is found to appear in the wave height of tsunamis. This is mainly because the dynamic ground displacement can be sometimes two or three times larger both in the amplitude and in the extent of the wave source area than the static one.
(2) Vertical ground displacement associated with Rayleigh waves induces another type of sea wave having velocity higher than the tsunami. It has special characteristics such as directivity and large velocity, and its amplitude depends on fault parameters and water depth.
(3) Employing a seismic fault model, the 1993 Hokkaido-Nansei-oki tsunami can be simulated to a satisfactory level of accuracy by means of the dynamic analysis.
(4) Sea surface disturbance that was not observed at Rumoi station but observed at Esashi and Iwanai stations in prior to the first tsunami is probably the sea wave induced by Rayleigh wave.
(5) Applying present approach, we have found a good agreement between the simulation and the observation at the western coast of Okushiri Island and the southwestern coast of Hokkaido.

REFERENCES

Hashimoto, M., S. Ozawa, A. Yoshimura, T. Sagiya, T. Tada, and H. Tsuji (1994) : Crustal movements associated with the 1993 Southwestern off Hokkaido earthquake and its fault model, Kaiyo Monthly, Special Edition for the Hokkaido Nansei-Oki Earthquake and Tsunamis, pp.55-61 (in Japanese).

Kakehi, Y. and K. Irikura (1997): High-frequency radiation process during earthquake faulting - Envelope inversion of acceleration seismograms from the 1993 Hokkaido-Nansei-Oki, Japan, earthquake, Bull. Seism. Soc. America, Vol.87, pp.901-917.

Mendoza, C. and E. Fukuyama (1996): The July 1993 Hokkaido-Nansei-Oki, Japan, earthquake: Coseismic slip pattern from strong-motion and teleseismic recordings, J. Geophys. Res., Vol. 101, pp.791-801

Ohmachi, T. and T. Nakama (1997): Numerical analysis on tsunami propagation produced by dynamic seismic faulting, Proc. of Coastal Eng. in Japan, JSCE, Vol.45, pp.311-314 (in Japanese).

Shuto, N. and H. Matsutomi (1995): Field Survey of the 1993 Hokkaido Nansei-Oki earthquake tsunami, PAGEOPH, Vol. 144, pp.649-663.

Takahashi, To., M. Oritz, Ta. Takahashi, and N. Shuto (1994) : Initial profile of the Hokkaido Nansei-oki earthquake tsunami for a better simulation, Progr. Abstr. Seism. Soc. Japan, C11-11 (in Japanese).